Int. J. Heat Mass Transfer. Vol. 29, No. 10, pp. 1531–1541, 1986
Printed in Great Britain

0017-9310/86 $3.00+0.00
Pergamon Journals Ltd.

Experimental determination of the behaviour of wet porous beds in which natural convection occurs

D. J. CLOSE and M. K. PECK

Division of Energy Technology, Commonwealth Scientific and Industrial Research Organization,
P.O. Box 26, Highett, Victoria 3190, Australia

(*Received* 22 *January* 1986 *and in final form* 5 *May* 1986)

Abstract—A theory developed previously has shown that a similarity relationship can be formed between natural convection heat transfer in a porous bed with a single fluid, and a similar system where the particles are wet and the interstitial mixture contains vapour and a second non-condensing gas. In this paper, data from a bed of glass spheres, bounded by horizontal, isothermal plates and with several gas and vapour mixtures, is reported. The enhancement in heat transfer rates forecast by the theory for large increases in gas to vapour molecular weight differences is shown by comparing water/air and water/Freon 12. The decrease in heat transfer rates forecast by the theory when the gas molecular weight is less than that of the vapour, is shown by comparing ethanol/air and ethanol/Freon 12. The validity of the similarity relationship is established by comparing these data plus a set from a different apparatus, with data for a water saturated bed of glass spheres. Heat transfer rates from the ethanol/air experiment are higher than predicted from models of heat transfer in stagnant packed beds. It appears that the system may be convecting in spite of an unfavourable density gradient.

1. INTRODUCTION

THIS paper describes results obtained from a study of natural convection in porous beds when the surfaces of the particles are wetted with a liquid and the pores are filled with a mixture of the liquid vapour and a second non-condensing gas.

Interest in this phenomenon arose from a desire to increase the charge and discharge rates of packed-bed thermal energy stores [1].

The conventional two-dimensional model of the system is shown in Fig. 1, and the apparatus to achieve it is shown in Fig. 2. To ensure that the particles are wet, a pool of liquid is maintained at the bottom where the heating surface is located. While Figs. 1 and 2 show horizontal cooling surfaces at the top, this is not a necessity. However, the liquid supply should be located at the highest temperature point or surface to ensure that condensation on all the particle surfaces can occur. An alternative method would be to spray or in some other way ensure that the particle surfaces are wet.

The simple method used to achieve wet porous beds means that the phenomenon may occur elsewhere, for example in partially saturated soils, offshore gas wells and the like. It may also have relevance to heat transfer in wet insulation and to moisture movement in grains and other adsorbing materials.

To date, a theory of the behaviour of these beds has been developed [2] and support for its conclusions has been provided by Davidson[3], who has solved a set of equations similar to the model in ref. [2] and also shown the effects of the variable system properties on the critical Rayleigh number, and the flow and temperature fields. Further verification has been sought from experimental data and the procedure adopted and results from the experiments are the subject of this paper.

2. THEORY

The theory developed for this physical system has been presented elsewhere [2], so that only a summary will be given here.

A simple model of natural convection in a porous medium saturated with a single-phase fluid is well known (see for example Combarnous and Bories [4])

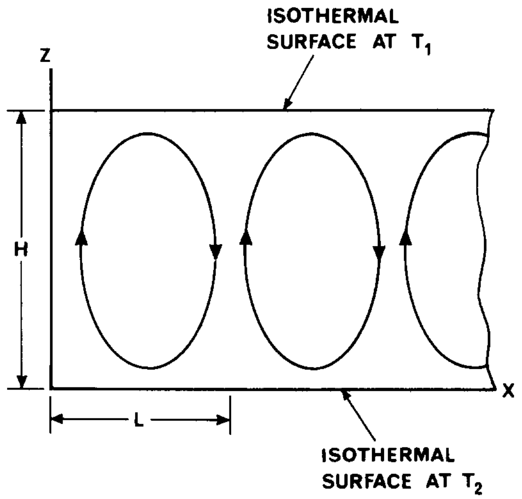

FIG. 1. Diagram of system used to analyse natural convection in porous media.

NOMENCLATURE

C_d	specific heat of non-condensing component or of single fluid $[\mathrm{J\ kg^{-1}\ K^{-1}}]$
C_K	Kozeney–Carman constant [—]
C_l	specific heat of liquid $[\mathrm{J\ kg^{-1}\ K^{-1}}]$
C^*	equivalent specific heat defined in equation (7) $[\mathrm{J\ kg^{-1}\ K^{-1}}]$
c	concentration of condensing component $[\mathrm{kg\ m^{-3}}]$
D	diffusivity of gas/vapour mixture $[\mathrm{m^2\ s^{-1}}]$
D^*	diffusivity of gas/vapour mixture in packed bed $[\mathrm{m^2\ s^{-1}}]$
d_h	hydraulic diameter of flow passages in packed bed [m]
g	gravitational acceleration $[\mathrm{m\ s^{-2}}]$
H	height of packed bed [m]
h	enthalpy of gas/vapour mixture, per unit mass of non-condensing component $[\mathrm{J\ kg^{-1}}]$
h_{fg}	latent heat of vaporization $[\mathrm{J\ kg^{-1}}]$
h_l	enthalpy of liquid $[\mathrm{J\ kg^{-1}}]$
k	effective conductivity of packed bed $[\mathrm{W\ m^{-1}\ K^{-1}}]$
k^*	effective conductivity of stagnant packed bed with no mass transfer $[\mathrm{W\ m^{-1}\ K^{-1}}]$
k^{**}	effective thermal conductivity of packed bed with coupled mass transfer defined in equation (9) $[\mathrm{W\ m^{-1}\ K^{-1}}]$
L	convection cell horizontal dimension [m]
M_c	molecular weight of condensing component $[\mathrm{kg\ (kg\ mol)^{-1}}]$
M_d	molecular weight of non-condensing component $[\mathrm{kg\ (kg\ mol)^{-1}}]$
m	mass ratio of condensing to non-condensing component [—]
N	buoyancy ratio, $\beta_c \Delta c/\beta \Delta T$ [—]
Nu^*	Nusselt number with no mass transfer, k/k^* [—]
Nu^{**}	Nusselt number with coupled mass transfer, k/k^{**} [—]
O_z	total surface area in packed bed $[\mathrm{m^2}]$
R	universal gas constant $[\mathrm{J\ kg\ mol^{-1}\ K^{-1}}]$

Ra^*	Rayleigh number with no mass transfer, $g\beta(\rho C_d/\nu_m)(\kappa/k^*)\Delta TH$ [—]
Ra^{**}	Rayleigh number with coupled mass transfer, $g\beta'(\rho_d C^*/\nu_m)(\kappa/k^{**})\Delta TH$ [—]
Ra_c	critical Rayleigh number [—]
T	temperature [K]
T_0	reference temperature [K]
T_1, T_2	isothermal surface temperatures [K]
T'	$(T-T_1)/(T_2-T_1)$ [—]
u	superficial fluid velocity in x direction $[\mathrm{m\ s^{-1}}]$
u'	$\rho_m(C_p uH/k^*)$ [—]
u''	$\rho_d(C^* uH/k^{**})$ [—]
v	superficial fluid velocity $[\mathrm{m\ s^{-1}}]$
V_z	total void volume of packed bed $[\mathrm{m^3}]$
w	superficial fluid velocity in z direction $[\mathrm{m\ s^{-1}}]$
w'	$\rho_m(C_p wL/k^*)$ [—]
w''	$\rho_d(C^* wL/k^{**})$ [—]
x	horizontal coordinate [m]
x'	x/L [—]
z	vertical coordinate [m]
z'	z/H [—].

Greek symbols

β	coefficient of volumetric expansion $[\mathrm{K^{-1}}]$
β'	$\beta\{1-[m/(1+m)](M_c-M_d)h_{fg}/RT\}$ $[\mathrm{K^{-1}}]$
β_c	$-(1/\rho_m)(\partial\rho_m/\partial c)_T$ $[\mathrm{m^3\ kg^{-1}}]$
ε	void fraction [—]
ψ	streamfunction, $u' = \partial\psi/\partial z'$, $w' = -\partial\psi/\partial x'$ [—]
ψ'	streamfunction, $u'' = \partial\psi'/\partial z'$, $w'' = -\partial\psi'/\partial x'$ [—]
ν_m	kinematic viscosity of fluid or mixture $[\mathrm{m^2\ s^{-1}}]$
ρ	density $[\mathrm{kg\ m^{-3}}]$
ρ_d	density of non-condensing component in mixture $[\mathrm{kg\ m^{-3}}]$
ρ_m	density of mixture $[\mathrm{kg\ m^{-3}}]$
κ	permeability $[\mathrm{m^2}]$
Δc	concentration difference $[\mathrm{kg\ m^{-3}}]$
ΔT	T_2-T_1 [K]
ΔT_c	temperature difference corresponding to Ra_c [K].

and makes the assumptions

(i) The Boussinesq approximation holds.

(ii) Fluid and solid properties are constant and an isotropic effective bed conductivity k^* accounts for heat transfer by conduction within the medium.

(iii) $(\mathbf{v}\cdot\mathrm{grad})\mathbf{v}$ terms are neglected.

(iv) Darcy's law holds.

(v) Rate coefficients between fluid and solid are high enough to assume local temperature equality.

The resulting dimensionless equations for steady state, and with a streamfunction ψ introduced are,

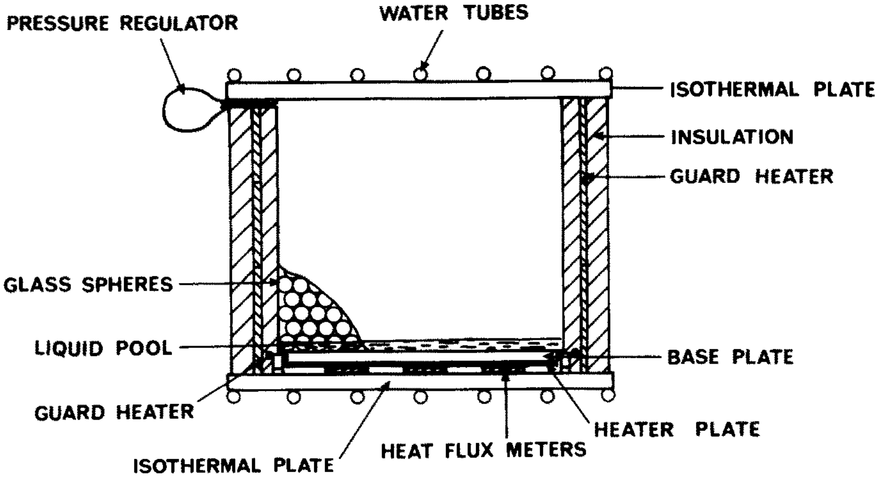

FIG. 2. Diagram of experimental apparatus.

from [5]

$$\left(\frac{H}{L}\right)^2\frac{\partial^2 T'}{\partial x'^2}+\frac{\partial^2 T'}{\partial z'^2}-\frac{H}{L}\left(u'\frac{\partial T'}{\partial x'}+w'\frac{\partial T'}{\partial z'}\right)=0 \quad (1)$$

$$\left(\frac{H}{L}\right)^2\frac{\partial^2 \psi}{\partial x'^2}+\frac{\partial^2 \psi}{\partial z'^2}+\frac{H}{L}Ra^*\frac{\partial T'}{\partial x'}=0. \quad (2)$$

For the case of isothermal boundaries as in Fig. 1, a Nusselt number is introduced with

$$Nu^* = \int_0^1 -\frac{\partial T'}{\partial z'}\,\mathrm{d}x'+\frac{H}{L}\int_0^1 w'T'\,\mathrm{d}x'. \quad (3)$$

While it is clear from data in refs. [4, 6, 7] that the dimensional groups Ra^* and H/L are insufficient to describe the process, and various authors, for example refs. [6–8] have attempted to improve the model, equations (1)–(3) form a useful starting point and conceptual framework for the phenomenon.

In a process where the particles are wet and the interstitial fluid is a mixture of vapour and a second non-condensing gas, then further assumptions are made. They are:

(vi) The fluid comprises an inert gas and a condensing vapour with perfect gas properties (for example air and water vapour), and the properties of the mixture and its components are assumed constant.
(vii) The surfaces of the packing are covered with liquid which flows vertically downwards through the packing and has no influence on the applicability of Darcy's law.
(viii) Following (v) above and Eckert and Faghri [9], there is local equality between the liquid vapour pressure and the vapour partial pressure, both equal to the vapour pressure of pure liquid at the local temperature.
(ix) The local liquid flow rate downwards equals the vapour flow rate upwards.

The last assumption is hard to justify since it takes no account of liquid flow mechanisms. Fortunately, liquid enthalpy flows are small compared with vapour enthalpy flows, so any errors introduced should be small.

Then, as shown in ref. [2], the conservation of energy and momentum yield

$$\left(\frac{H}{L}\right)^2\frac{\partial^2 T'}{\partial x'^2}+\frac{\partial^2 T'}{\partial z'^2}-\frac{H}{L}\left(u''\frac{\partial T'}{\partial x'}+w''\frac{\partial T'}{\partial z'}\right)=0 \quad (4)$$

$$\left(\frac{H}{L}\right)^2\frac{\partial^2 \psi'}{\partial x'^2}+\frac{\partial^2 \psi'}{\partial z'^2}+\frac{H}{L}Ra^{**}\frac{\partial T'}{\partial x'}=0 \quad (5)$$

and for the case of isothermal boundaries, a Nusselt number is introduced with

$$Nu^{**} = \int_0^1 -\frac{\partial T'}{\partial z'}\,\mathrm{d}x'+\frac{H}{L}\int_0^1 w''T'\,\mathrm{d}x'. \quad (6)$$

The new properties introduced are

$$C^* = \frac{\mathrm{d}h}{\mathrm{d}T}-h_l\frac{\mathrm{d}m}{\mathrm{d}T} \quad (7)$$

$$\beta' = \beta\left[1-\frac{m}{1+m}(M_c-M_d)\frac{h_{fg}}{RT}\right] \quad (8)$$

$$k^{**} = k^*+\frac{\rho_m^2}{\rho_d}D^*h_{fg}\frac{\mathrm{d}}{\mathrm{d}T}\left(\frac{m}{1+m}\right) \quad (9)$$

$$Ra^{**} = g\beta'\frac{\rho_d C^*}{\nu_m}\frac{\kappa}{k^{**}}\Delta T H. \quad (10)$$

It is clear that the equation set (1)–(3) resembles the set (4)–(6). However, several properties in the latter set show considerable variability with temperature: for example C^*, β' and k^{**}.

To use data from single fluid experiments, which are expressed in terms of equations (1)–(3), to forecast the behaviour of wet porous beds requires that the properties be constant, or nearly so. This implies that temperature differences across the wet porous bed should be small. The analysis by Davidson [3] indicates that the analogy holds for small temperature differences.

From the assumptions, it is clear that the gas/vapour mixture in the voids is saturated. Consequently C^* is easily obtained from the properties of saturated gas/vapour mixtures. From Obert [10], the mixture enthalpy h is given by

$$h = \int_{T_0}^{T} C_d \, dT + m\left[\int_{T_0}^{T} C_l \, dT + h_{fg}\right]$$

and since for a saturated mixture $m = m(T)$

$$\frac{dh}{dT} = C_d + m\left(C_l + \frac{d}{dT}h_{fg}\right) + \frac{dm}{dT}\left[\int_{T_0}^{T} C_l \, dT + h_{fg}\right].$$

The term $h_l(dm/dT)$ in C^* is a correction term for the liquid trickling back down the bed and, as shown in ref. [2], is relatively small compared with dh/dT. Since C^* accounts for the energy involved in evaporating and condensing vapour it is considerably larger than C_d, particularly near the liquid boiling point where it is in the order of h_{fg}.

The effective buoyancy β' includes the effect of the concentration variation on the mixture density. Of interest is the possibility of reversing the buoyancy forces depending on the molecular weights of the condensing and non-condensing components. If $M_c > M_d$, then a neutral buoyancy temperature exists. This separates buoyancy forces in one direction from buoyancy forces in the other. Phenomena such as this have been observed elsewhere, for example [11–14], but these studies have focused on boundary-layer cases rather than the packed beds where an assumption of the fluid mixture being saturated is appropriate. In principle, β' can be positive or negative and under certain conditions much larger than β for a gas mixture.

Of interest is the recent paper by Trevisan and Bejan [15] who investigate the simultaneous effects of concentration and temperature effects on natural convection in a porous bed. The imposed temperatures and concentrations are on the vertical boundaries, and the concentration and temperature are not coupled as is the case here. They show that convection is suppressed when $N = \beta_c \Delta c / \beta \Delta T = -1$. This corresponds to the neutral buoyancy case $\beta' = 0$ in (8) above.

The effective conductivity k^{**} includes the mass diffusion contribution $(\rho_m^2/\rho_d)D^* h_{fg}(d/dT)[m/(1+m)]$ and is well known in studies of moisture diffusion in porous media (see, for example, ref. [9]). This form differs from that used in ref. [2] where the gradient used was dm/dT and where ρ_m occurred instead of ρ_m^2/ρ_d. While a satisfactory approximation for low concentrations of vapour, use of the gradient dm/dT is inappropriate for high concentrations as occur near the vapour boiling point. The multiplier ρ_m^2/ρ_d occurs because with the interdiffusion of the gas and vapour, the problem resembles that dealt with by Eckert and Drake [16]. Vapour diffusion has a sink in that it condenses and flows down through the bed but there is no such sink for the non-condensing component. An effective velocity of the mixture is postulated, where the flow of the mixture counters the diffusion of the non-condensing component. This effective velocity of the mixture results in an increase in vapour diffusion which is reflected in the multiplier ρ_m^2/ρ_d as compared to ρ_m. k^{**} differs little from k^* at low concentrations of vapour but can be much larger near the vapour boiling point.

It should be noted that whereas in the definition of Ra^* the term ρC_p appears, the equivalent grouping in Ra^{**} is $\rho_d C^*$. As the temperatures in a bed approach the vapour boiling point, C^* increases but ρ_d decreases. Hence the product increases considerably more slowly than does C^*. However, values of $\rho_d C^*$ for air and water vapour are still around 200 times those for dry air at 90°C.

Some important conclusions from the theoretical study include:

(i) Significant increases in the effective conductivity under convecting conditions can be achieved using the same vapour but changing the non-condensing gas to one with a higher molecular weight. Conversely convection can be suppressed using a gas having a lower molecular weight than the vapour.

(ii) Convection generally occurs at much smaller temperature differences, lower bed heights, or smaller particle diameters with the wet porous bed case than for a single gas having the same density, viscosity and thermal conductivity.

(iii) Convection can occur in the upside down (hot top, cold bottom) mode with mixtures where the gas molecular weight is lower than that of the vapour.

The experimental program has dealt primarily with (i), and (ii) can be inferred from the results. Limitations in the experimental apparatus, in that a free or nearly free liquid surface could not be maintained at the top of the bed, prevented experiments verifying (iii) from being performed.

3. EXPERIMENTAL APPARATUS AND PROCEDURE

A diagram of the apparatus used is shown in Fig. 2. It is approximately a cube (300 mm side length), with water-heated and water-cooled plates at top and bottom, and guard heaters on the sides. At the base, the water-heated plate is separated from a 12.5-mm-thick aluminium base plate by three heat flux meters and thin cardboard having the same thickness as the meters, and an electric heating element encased in laminated plastic sheets. The element is supplied by a variable transformer.

The dimensions of the vessel were chosen so that glass spheres of about 29 mm diameter could be packed in an array as shown in Fig. 3. This allowed the geometry of the bed to be specified.

To keep the system at constant pressure an

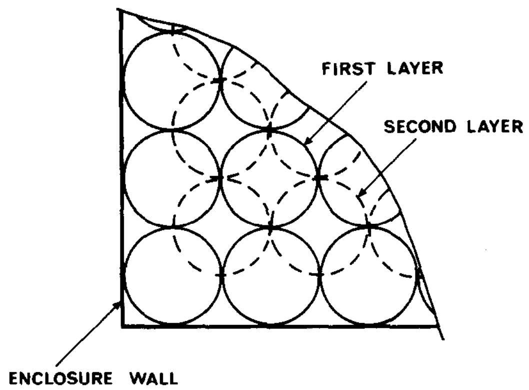

FIG. 3. Diagram showing packed bed array geometry viewed from above.

aluminized plastic bag was connected to a tube at the top of the container. As the volume increased with the increased temperature in the container, the bag inflated and if necessary, gas was released from it. Liquid was added to the container through a tube connected at the bottom.

The guard heaters were three independent heating pads separated from the container walls by 25 mm of insulation, and mounted on an aluminium sheet which was slotted to isolate one zone from the other. One further guard heater, a single wire, was located on the extension block of the lower isothermal plate (see Fig. 2). The heaters were controlled by differential controllers sensing the difference between the container wall and the guard plate. Measurements showed these differences to be of the order of 0.4°C.

To perform the experiments, the liquid to be used was poured into the base of the container and the level measured. Then the gas to be used, if other than air, was introduced. If lighter than the gas in the container it was introduced from the top; if heavier than the gas in the container, it was introduced into the bottom. When Freon 12 was the gas to be used, it was slowly bled into the container and a Freon 12 detector placed at the outlet tube. When the detector suddenly indicated a high concentration of Freon 12, the introduction of the gas was continued for a further 5 min. In the case of air displacing Freon 12, the detector was used and the vessel was assumed full of air when no Freon 12 could be detected.

The apparatus was also checked by comparing the *Nu* vs *Ra* relationship using only air and without spheres. The measured data are shown in Fig. 4 compared with the data of Buchberg *et al.* [17] and the correlation of Hollands [18]. The agreement with ref. [17] is within 5%, and also agrees to within 5% with independent measurements made at our laboratory by Lam [19].

4. EXPERIMENTAL METHOD

Following placement of the spheres, gas and liquid in the container, a pair of hot and cold plate temperatures and the power input were chosen, estimates of these being made using the theory given in Section 2.

A maximum output of the three heat flux meters connected in series of 100 μV, was used as a guide to

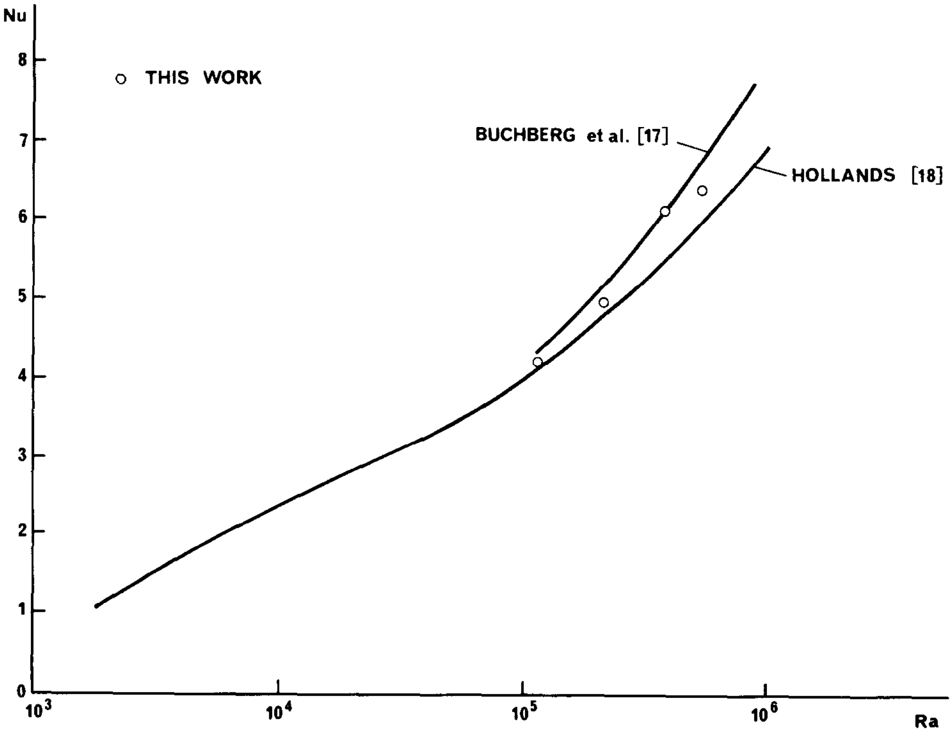

FIG. 4. Experimental data from apparatus compared with results from Buchberg *et al.* [17] and Hollands *et al.* [18].

when satisfactory stability had occurred. This corresponds to a flux of 0.02 W between the heater plate and the water heated plate, considering the relative thermal conductivities of the heat flux meters and cardboard. The final tuning of the apparatus to steady state was achieved by adjusting the temperature of the water bath supplying the hot plate. Adjustments of the order of 0.001°C could be obtained.

Steady state was assumed and the experiment terminated when over a period of 1 h the heat flux meter output remained within the bounds described above, or an adjustment of 0.001°C produced a change from a negative to a positive output over the same period. In the second case, sometimes used to speed up the equilibrating process, the difference between the two effective conductivities measured was negligible, being of the order of 1%.

Measurements of thermocouple output and heater voltage were made on calibrated digital voltmeters, and the thermocouple wire had been calibrated prior to the experiments.

The uncertainties in temperature are ±0.1 K and in heater power, 0.03 W.

5. EXPERIMENTAL RESULTS

Four gas/vapour mixtures were used in the experiment, namely water/air, water/Freon 12, ethyl alcohol azeotrope/Freon 12 and ethyl alcohol azeotrope/air.

The measured effective bed thermal conductivities are plotted in Fig. 5 as functions of the mean bed temperature $\bar{T}$. As shown later, the data can be condensed onto a Nusselt number vs Rayleigh number plot, but some important points can be drawn from Fig. 5.

The comparison between the water/air and water/Freon 12 data sets clearly shows the effect of changing the gas molecular weight. The temperature differences used for the water/Freon 12 mixture were in the approximate range 7.4–12.4 K whereas the range for the water/air mixture was approximately 9.3–10.4 K. Hence the difference cannot be explained by using different temperature differences in the two cases. In changing the non-condensing gas from air to Freon 12, the theory developed in ref. [2] predicted a large increase in k and this is observed, the primary reason being the change in the effective buoyancy β' and the decrease in the mixture viscosity.

In the case of the ethyl alcohol–water azeotrope with either air or Freon 12, the theory predicts suppression of convection with air but not with Freon 12. While some doubt exists, as discussed in later sections, as to whether complete suppression has occurred when using air, a very large reduction is shown.

The large increase in conductivity as the mixture approaches the vapour boiling point for three of the cases was forecast in ref. [2] and is attributed primarily to the increases in β' and C^* with temperature.

Of interest is the temperature difference at which convection would occur in the same bed and with a gas having the same density, viscosity and thermal conductivity as the saturated mixtures used, and a specific heat corresponding to a change in mixture

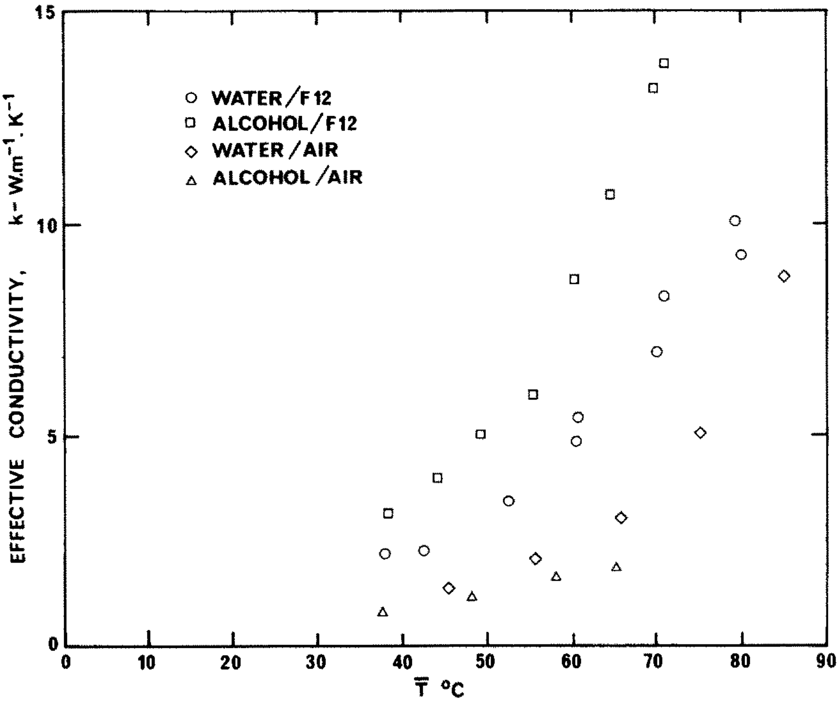

FIG. 5. Measured effective conductivities of a bed of glass spheres saturated with various gas/vapour mixtures.

Table 1. Temperature differences ΔT_c corresponding to Ra_c for gas mixtures but no mass transfer

Mixture	ΔT_c (K)
Air/water	128
Freon 12/water	18.9
Air/ethyl alcohol	3.9
Freon 12/ethyl alcohol	4.7

temperature only. Assuming a value of $4\pi^2$ for the critical Rayleigh number, then the corresponding values of ΔT are shown in Table 1 for a mean temperature of 70°C.

Particularly in the case of the air/water vapour mixture and for Freon 12/water, the evidence from Fig. 5 indicates very strongly that both are convecting whereas from Table 1 there would be no convection with no evaporation. Note that the temperature differences used in the experiment varied between 7.4 and 12.4 K. For Freon 12/ethyl alcohol only weak convection corresponding to Rayleigh numbers of 2 or 3 times critical should occur, whereas Fig. 5 again shows strong convection. The case of air/ethyl alcohol is of course different as discussed earlier, in that convection is not expected to occur in this case.

6. ANALYSIS OF RESULTS AND DISCUSSION

The theory presented in ref. [2] and summarised in Section 2 above requires that the modified Rayleigh number Ra^{**} be determined.

The azeotrope was assumed to be ethyl alcohol only in these calculations.

The basic fluid properties were obtained from refs. [20, 21]. In the case of the mixture viscosity and conductivity these were calculated from the method in Bird *et al.* [22], and for the diffusivities of the water/Freon 12, alcohol/Freon 12 and alcohol/air, a procedure in ref. [20] was employed. For Freon 12 only, a compressibility function was determined from properties of the saturated gas, and the buoyancy β' determined from the basic relationship

$$\beta' = -\frac{1}{\rho_m}\frac{d\rho_m}{dT}$$

rather than from (8). All other gases and vapours were assumed perfect. All properties were curve fitted to better than 1% accuracy using polynomial fits, except for those cases where curve fits already existed.

The value of k^{**} used to normalise both Nu^{**} and Ra^{**} was calculated from (9) using a value of $D^* = 0.2D$ where D is the diffusivity for the gas vapour pair, for example, see Eckert and Faghri [9].

To calculate the permeability the method employed is that given by Schneider [26] with

$$\kappa = \tfrac{1}{16}\varepsilon\frac{d_h^2}{C_k}$$

where $d_h = 4V_z/O_z$ and $C_k = 4.94$. This was used by Buretta [24] and Close *et al.* [27].

One further piece of data required was the quantity of liquid. The assumption was made that all the liquid remained in the bottom of the container, and this allowed the height of liquid, the net height of the bed, surface area and finally the permeability to be determined. How valid this assumption is, is presently not known.

Plots of Nu^{**} vs Ra^{**} for three of the mixtures used are shown in Fig. 6. Values taken from a separate and much larger apparatus using the same glass spheres and with air/water as the mixture are also shown. This experiment, described elsewhere [23] was performed in a 1.75-m-diameter, 0.5-m-high cylinder and with a lower boundary condition closer to a constant flux than isothermal surface, and lends support to the results presented here. These data have been recalculated for this paper using (9) for k^{**}. In ref. [23], ρ_m rather than ρ_m^2/ρ_d was used in the vapour diffusion term.

If the similarity hypothesis advanced in Section 2 has validity, then the data should resemble those for a heat transfer only case. That this is so, is shown by the comparison between these data and data from Buretta [24] for glass spheres and liquid water.

There is not complete agreement between the three gas/vapour mixtures when the results are plotted in this way, since the theory in Section 2 requires much further refinement. Also there will be some effect from assuming that the azeotrope was alcohol only. However, the scatter in data is no greater than has been observed in heat transfer only cases, for example as shown in the data of Combarnous [25] in liquid-saturated beds. The situation regarding the alcohol/air case is of interest as the bed should have been stagnant during this series of experiments. However when the conductivity calculated according to equation (9) is compared with the data, then a significant discrepancy occurs. This is shown in Fig. 7.

Higher effective bed conductivities can be explained by two mechanisms, both plausible in this context. There will be liquid menisci between the particles, so increasing the thermal conductance between them as compared to the situation where gas only exists. Further, the menisci may not be stagnant.

To see whether these mechanisms can explain the discrepancy between (9) and the data, k^{**} has been recalculated for the extreme case of no interparticle resistance. As shown in Fig. 7, this does not explain the high conductivities above about 50°C. However, if the interparticle resistance is a function of the vapour diffusion rate, increasing as the mean temperature increases, then improved agreement between theory and experiment can be obtained.

Other possible causes for the discrepancy, are the non-linear nature of the conduction process due to the variability of k^{**} with temperature and the influence of experimental errors. Neither are large enough to explain the difference and, as shown in Fig. 8, the

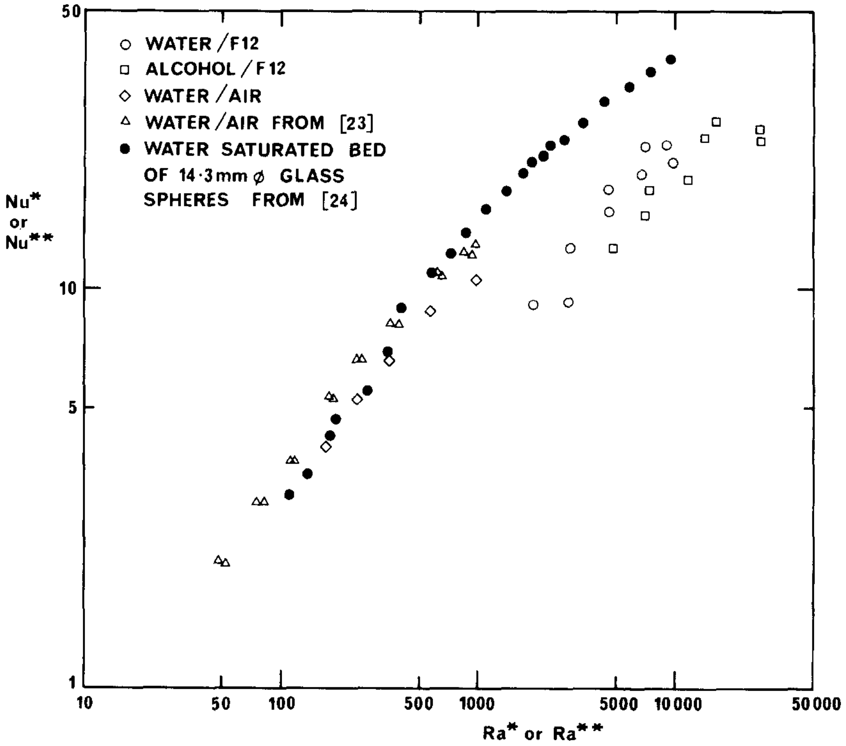

FIG. 6. *Nu*** vs *Ra*** data for a bed of glass spheres saturated with various gas/vapour mixtures, compared with *Nu** vs *Ra** data for a water saturated bed of glass spheres from ref. [24].

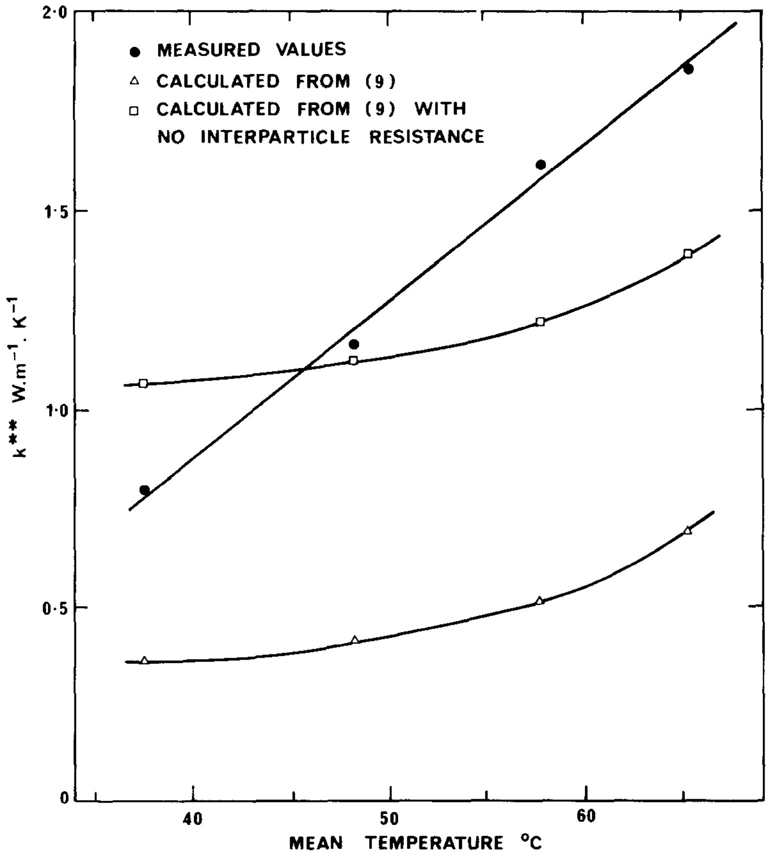

FIG. 7. Measured effective thermal conductivity of a bed of glass spheres saturated with an alcohol/air mixture compared with various conduction models.

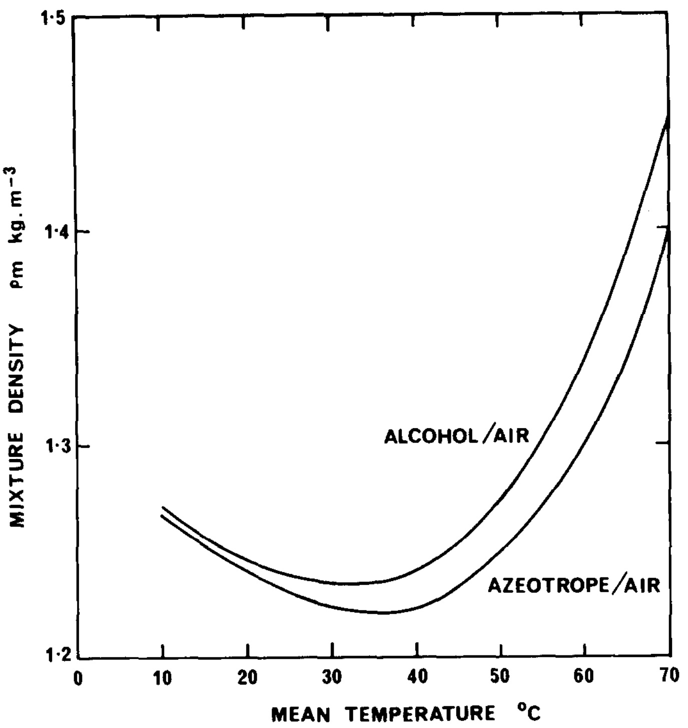

FIG. 8. Calculated values of the densities of saturated mixtures of ethyl alcohol/air and ethyl alcohol and water azeotrope/air as functions of temperature. Mixture pressure 1 atm.

densities of azeotrope/air and pure ethyl alcohol/air mixtures are nearly the same so use of the azeotrope is not a likely cause.

Whether the explanation lies in deficiencies in the stagnant conduction model or in the assumption of stagnant conditions is not presently known and further work is obviously necessary here.

Of some concern is the use of k^{**} from equation (9) in the normalisation of Nu^{**} and Ra^{**}.

If the effective stagnant conductivity is not adequately described by (9), then some changes occur in the plots in Fig. 6, with the slopes of the curves somewhat lower but the points remaining almost unaffected near values of $Nu^{**} = 1$.

Sufficient work has been done on beds saturated with a single fluid, to show that the simple model contained in equations (1) and (2) is not a complete description of the process, for example refs. [4–8]. It is certain that similar inadequacies will apply in this coupled mass transfer case. A more detailed theory is presently being developed.

7. CONCLUSIONS

The primary thrust of this work was to provide support for the theory advanced in ref. [2].

The predicted trends have been followed, particularly those relating to the effect of relative molecular weights of gas and vapour and mixture properties, on the total heat transfer rate.

In addition, there is very good agreement between these data and Nu^* vs Ra^* data for water-saturated beds of glass spheres further supporting the general validity of the similarity relationships in equations (4)–(6).

Presently the results for the alcohol water azeotrope/air mixture cannot be explained in terms of the models used to set up the theory. The most likely explanation for this is that convection persists even though the buoyancy forces appear to ensure stagnant conditions.

A more sophisticated apparatus is being constructed, able to answer more of these questions.

Acknowledgements—The authors are grateful for advice and assistance from their colleagues Dr J. G. Symons of the Division of Energy Technology and R. Gani of the Department of Mechanical Engineering, Monash University. Thanks are also tendered to R. G. Hiskins and Ms J. Lessig for help in setting up the experiments and recording data.

REFERENCES

1. D. J. Close and M. K. Peck, High temperature thermal energy storage: a method of achieving rapid charge and discharge rates, *Sol. Energy* (in press).
2. D. J. Close, Natural convection with coupled mass transfer in porous media, *Int. Commun. Heat Mass Transfer* **10**, 465–476 (1983).
3. M. R. Davidson, Natural convection of gas/vapour mixtures in a porous medium, *Int. J. Heat Mass Transfer* **29**, 1371–1381 (1986).
4. M. A. Combarnous and S. A. Bories, Hydrothermal convection in saturated porous media, *Adv. Hydrosci.* **10**, 231–307 (1975).

5. K. Aziz, P. H. Holst and P. S. Karra, Natural convection in porous media, Petrol. Soc. Can. Inst. Mining, Calgary, Paper 6813 (1968).
6. V. Prasad, F. A. Kulacki and M. Keyhani, Natural convection in porous media, *J. Fluid Mech.* **150**, 89–119 (1985).
7. D. J. Close, A general correlation for natural convection in liquid saturated beds of spheres, *J. Heat Transfer* (in press).
8. Y. T. Chan and S. Banerjee, Analysis of transient three-dimensional natural convection in porous media, *J. Heat Transfer* **103**, 242–248 (1981).
9. E. R. G. Eckert and M. Faghri, A general analysis of moisture migration caused by temperature differences in an unsaturated porous medium, *Int. J. Heat Mass Transfer* **23**, 1613–1623 (1980).
10. E. F. Obert and R. L. Young, *Elements of Thermodynamics and Heat Transfer*. McGraw-Hill, New York (1962).
11. T. S. Lee, P. G. Parikh, A. Acrivos and D. Bershader, Natural convection in a vertical channel with opposing buoyancy forces, *Int. J. Heat Mass Transfer* **25**, 499–511 (1982).
12. W. N. Gill, E. Del Casal and D. W. Zeh, Binary diffusion and heat transfer from a vertical plate, *Int. J. Heat Mass Transfer* **8**, 1135–1151 (1965).
13. B. Gebhart and L. Pera, The nature of vertical natural convection flows resulting from the combined buoyancy effects of thermal and mass diffusion, *Int. J. Heat Mass Transfer* **14**, 2025–2050 (1971).
14. J. A. Adams and R. L. Lowell Jr., Free convection organic sublimation, *Int. J. Heat Mass Transfer* **11**, 1215–1224 (1968).
15. O. V. Trevisan and A. Bejan, Natural convection with combined heat and mass transfer buoyancy effects in a porous medium, *Int. J. Heat Mass Transfer* **28**, 1597–1611 (1985).
16. E. R. G. Eckert and R. M. Drake, *Heat and Mass Transfer*. Krieger, New York (1959).
17. H. Buchberg, I. Catton and D. K. Edwards, Natural convection in enclosed spaces—a review of applications to solar energy collection, *J. Heat Transfer* **98**, 182–188 (1976).
18. K. G. T. Hollands, G. D. Raithby and L. Konicek, Correlation equations for free convection heat transfer in horizontal layers of air and water, *Int. J. Heat Mass Transfer* **18**, 879–884 (1975).
19. S. Lam, Department of Mechanical Engineering, Monash University, Personal communication.
20. W. M. Rohsenow and J. P. Hartnett, *Handbook of Heat Transfer*. McGraw-Hill, New York (1973).
21. *Handbook of Chemistry and Physics*. The Chemical Rubber Company, OH (1969).
22. R. B. Bird, W. E. Stewart and E. L. Lightfoot, *Transport Phenomena*. Wiley, New York (1960).
23. D. J. Close and M. K. Peck, Some effects of natural convection in wet porous beds, *Third Australasian Conference on Heat and Mass Transfer*, Melbourne, pp. 161–168 (May 1985).
24. R. A Buretta, Thermal convection in a fluid filled porous layer with uniform internal heat sources. Ph.D. thesis, University of Minnesota (1972).
25. M. Combarnous, Convection naturelle et convection mixte en milieu poreux. Thesis, University of Paris (1970).
26. K. J. Schneider, Die Warmeleitfahigkeit korniger stoffe und ihre Beeinflussung durch freie Konvektion. Thesis, University of Karlsruhe (1963).
27. D. J. Close, J. G. Symons and R. F. White, Convective heat transfer in shallow, gas-filled porous media: experimental investigation, *Int. J. Heat Mass Transfer* **28**, 2371–2378 (1985).

DETERMINATION EXPERIMENTALE DU COMPORTEMENT DE LITS POREUX HUMIDES A L'INTERIEUR DESQUELS REGNE LA CONVECTION NATURELLE

Résumé—Une théorie développée précédemment a montré qu'une relation de similitude peut être établie entre le transfert par convection naturelle dans un lit poreux avec un fluide unique et un système semblable où les particules sont humides et le mélange intersticiel contient de la vapeur et un gaz non condensable. Dans cet article, on décrit des expériences avec un lit de sphères de verre limité par des plaques horizontales et isothermes et avec quelques mélanges de gaz et de vapeur. L'accroissement de transfert thermique prévu par la théorie pour des grandes différences de masses moléculaires de la vapeur et du gaz est montré en comparant vapeur d'eau/air et vapeur d'eau/Freon 12. La décroissance du transfert thermique prévue par la théorie quand la masse moléculaire du gaz est moindre que celle de la vapeur est montrée en comparant ethanol/air et ethanol/Freon 12. La validité de la relation de similitude est établie en comparant des données, et celles obtenues, avec un appareil différent, avec des données pour un lit de sphères de verre saturé d'eau. Les flux thermiques dans l'expérience éthanol/air sont plus grands que prévus par les modèles de lits fixes stagnants. Il apparait que le système peut être convectant en dépit d'un gradient défavorable de masse volumique.

NATÜRLICHE KONVEKTION IN FLÜSSIGKEITSGESÄTTIGTEN PORÖSEN BETTEN

Zusammenfassung—Eine früher entwickelte Theorie zeigte die Möglichkeit zur Formulierung einer Ähnlichkeitsbeziehung für den Wärmetransport bei natürlicher Konvektion einerseits in einem porösen Bett, welches ein reines Fluid enthält, und einem ähnlichen System andererseits, bei dem die Partikel benetzt sind und sich in den Zwischenräumen Dampf und ein zweites nicht kondensierendes Gas befinden. In dieser Arbeit werden Ergebnisse für ein mit horizontalen isothermen Platten abgegrenztes Bett aus Glaskugeln mit unterschiedlichen Gas- und Dampfgemischen vorgestellt. Die mit der Theorie abgeschätzte Erhöhung des Wärmeübergangs für ein großes Anwachsen des Unterschieds zwischen den Molekulargewichten von Gas und Dampf wird durch einen Vergleich der Gemische Wasser/Luft und Wasser/Freon 12 gezeigt. Das mit der Theorie vorhergesagte Absinken des Wärmeübergangs, wenn das Molekulargewicht des Gases kleiner ist als das des Dampfes, wird durch den Vergleich der Gemische Äthanol/Luft und Äthanol/Freon 12 gezeigt. Die Gültigkeit der Ähnlichkeitsbeziehung wird durch einen Vergleich der Ergebnisse bestätigt, welche an dieser und einer anderen Anlage mit Daten für ein wassergesättigtes Glaskugelbett ermittelt worden sind. Die gemessenen Wärmeübergangskoeffizienten beim Äthanol/Luft-Experiment sind höher als die für ruhende Festbetten berechneten. Es scheint, daß das System ungeachtet eines ungünstigen Dichtegradienten eine Konvektionsbewegung ausführt.

ЕСТЕСТВЕННАЯ КОНВЕКЦИЯ ВО ВЛАЖНЫХ ПОРИСТЫХ СЛОЯХ

Аннотация—Ранее теоретически было показано, что можно провести аналогию между теплопереносом естественной конвекцией в пористом насыщенном однофазной жидкостью слое и аналогичной системой, содержащей влажные частицы, промежутки между которыми заполнены смесью из пара и неконденсирующегося газа. Приводятся результаты опытов со слоем из стеклянных шариков, ограниченного горизонтальными изотермическими пластинами, и смесями из газа и пара. Предсказанное теорией возрастание интенсивности теплообмена при увеличении разности между молекулярными весами газа и пара иллюстрируется на примере систем вода–воздух и вода–Фреон 12. Снижение интенсивности теплообмена, рассчитанное теоретически для случая, когда молекулярный вес газа меньше, чем у пара, подтверждается экспериментами с системами этанол–воздух и этанол–Фреон 12. Из сравнения этих данных и данных, полученных для других систем, с результатами экспериментов со слоем стеклянных шариков, насыщенным водой, установлен критерий подобия. Интенсивность теплообмена в опытах с системой этанол–вода выше значения, рассчитанного из модели теплообмена в неподвижных плотных слоях. Повидимому, несмотря на отрицательный градиент плотности, в такой системе может иметь место конвективное движение.